

# **DEVELOPMENT OF NB BEARING HIGH STRENGTH STEEL FOR BUILDINGS BY MICROSTRUCTURAL CONTROL THROUGH THE ON-LINE HEATING PROCESS**

Shinichi Suzuki, Keiji Ueda  
JFE Steel Corporation; Steel Research Lab., Kawasaki 210-0855, JAPAN  
Shinji Mitao, Nobuo Shikanai  
JFE Steel Corporation, Steel Research Lab., Kurashiki 712-8511, JAPAN  
Takayuki Ito  
JFE Steel Corporation, West Japan Works, Fukuyama 721-8510, JAPAN

**Keywords:** Building Structure, Deformability, Dual-Phase, martensite-austenite (M-A)

## **Abstract**

This paper presents and discusses the development of high strength steel plates with 780MPa in tensile strength that are suitable for building construction use. Such plates provide an excellent combination of high strength, toughness, deformability and weldability. The key technology to obtain the excellent combination in mechanical properties is the microstructural control of the martensite-austenite (M-A) constituent and the bainitic ferrite dual-phase structure through on-line heat treatment immediately after accelerated cooling during Thermo-Mechanical Controlled Processing (TMCP).

The developed steel plates exhibit microstructures of fine M-A dispersed in the bainitic ferrite matrix and basic metallurgical investigations revealed that the transformation behaviour and microstructural morphologies were varied with the cooling step temperatures before the on-line heating and the on-line heating temperature itself. The paper also briefly discusses the trial production of the developed 780MPa grade steel plate which demonstrated satisfactory combinations of high strength, low yield ratio, toughness and weldability.

## **Introduction**

The recent increased demands for larger-scale and longer-span design in high-rise buildings have promoted the application of high strength steels for building construction [1-5]. In response to these demands, JFE Steel has developed a series of high performance steel products for buildings as shown in Figure 1. So far, the tensile strength of steel plates applied for building construction in Japan is typically up to 590MPa (440MPa in the yield stress), due to many restricting factors such as price and weldability. To provide resistance to fracture during earthquakes, the low yield ratio (yield stress / tensile strength), typically lower than 80%, is preferable to steel plates for building construction [6,7], as registered in Japanese Industrial Standards (JIS G 3136). However, it is quite difficult to obtain low yield ratio in high strength steels, even in the 590MPa grade steel plate. Complex multiple heat treatments in the manufacturing process to achieve low yield ratios results in an increase in production cost and prolong delivery times.

To prevent these problems, JFE Steel developed 550MPa (385MPa in the yield stress) grade steel plate, “HBL385” [8,9]. Although the yield stress and tensile strength of the developed

steel is higher than 520MPa grade steel by 30MPa, the carbon equivalent (Ceq) is same as those of 520MPa grade steel. This is achieved by the application of Thermo-mechanical control process (TMCP) with “Super-OLAC”, an advanced accelerated cooling system [10, 11], and by the addition of Nb without any heat treatment. Therefore, the weldability of the developed 550MPa grade steel is equal to that of 520MPa grade steel, and it is possible to reduce the welding cost in steel frame fabrication compared with that of 590MPa grade steel. Accordingly, in comparison with the conventional grade steels, such as 520MPa grade and 590MPa grade steels, the total fabrication cost of the steel frame is minimized by the reduction of steel weight, welding time, transportation cost and easiness of welding procedures. Figure 2 shows an example of frame fabrication cost ratio and steel weight ratio with the variation of steel grade. As the superiority of “HBL385” has been highly evaluated, it is now widely used in prestigious large buildings in Japan.

Tensile strength	400MPa class	490MPa class	520MPa class	550MPa class	570MPa class	590MPa class	780MPa class
Steels for general welded structure (JIS)	SM400	SM490	SM520		SM570		SHY685
Steels for building structure with low YR	↓	↓	↓	Earthquake resistance Lowering yield ratio		↓	↓
	SN400	SN490	SM520N			SA440	
		↓	↓	Applying TMCP technology Improvement of weldability			↓
		HBL325	HBL355	HBL385			Low YR HT780

Figure 1. Series of steel plates for buildings in JFE Steel.

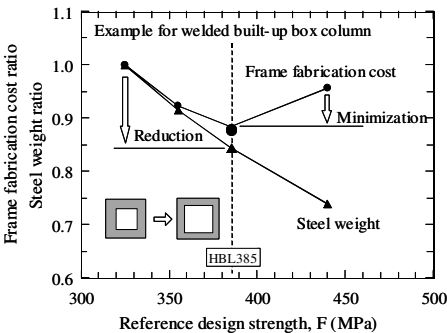


Figure 2. An example of frame fabrication cost ratio and steel weight ratio with a variation of steel grade (SN490 = 1.0).

Where higher strength steel is necessary, 780MPa grade steel is very effective; however there have been few applications of this grade steel. One of the reasons is that the complex multiple heat treatments are a necessity for manufacturing 780MPa grade steel plates with a low yield ratio. In addition, since greater amounts of alloying elements are added to obtain higher strengths, not only the alloy cost, but also toughness and weldability are intrinsic problems to be solved for commercial products.

In this study, high strength steel plates with 780MPa in tensile strength by the on-line process

without any off-line heat treatments have been developed. The developed steel plates show excellent combination of high strength, toughness, low yield ratio and weldability. The key technology to obtain the excellent combination in mechanical properties of the steel is the microstructural control of M-A (martensite-austenite) constituent and the bainitic ferrite dual-phase structure [12-17], through the on-line heating immediately after the accelerated cooling in TMCP. The heat treatment on-line process, “HOP”, enables microstructural control [11]. “HOP” is the induction heating device installed next to the accelerated cooling as described in previous literatures [18,19]. The resultant steel plates have a microstructure of fine M-A particles dispersed in the bainitic ferrite matrix.

Effects of manufacturing conditions, such as the cooling stop temperature before the on-line heating, and the on-line heating temperature, on microstructural characteristics and the resultant mechanical properties have been investigated systematically. Formation mechanism of the M-A and bainitic ferrite dual-phase structure, and morphological changes in the microstructure depending on the manufacturing conditions was discussed in terms of concentration of carbon into the untransformed austenite during the on-line heating after accelerated cooling.

### Experimental Procedures

#### Chemical composition and CCT diagram

The chemical composition of the steel employed is given in Table 1. The steel contains 0.06% of carbon, 2% of manganese, and small amount of other alloying elements, such as Cu, Ni, Cr, Nb, V and Ti. These alloying elements are added to achieve high strength and excellent toughness. The steel ingot of about 150kg in weight was prepared by a laboratory scale induction melting furnace. The obtained ingot was hot-rolled to 100mm in thickness. Samples for thermal cycle tests and hot-rolling tests were taken from the 100mm-thick slab.

Figure 3 shows the continuous cooling transformation (CCT) diagram for the steel after hot deformation. The bainite transformation starting temperature (Bs) was changed from about 400 to 600°C with a decrease in the cooling rate from 40 to 0.5°C/s.

Table 1. Chemical composition of the steel studied.

C	Si	Mn	P	S	Others
0.061	0.20	2.03	0.012	0.0020	Cu, Ni, Nb, V, Ti

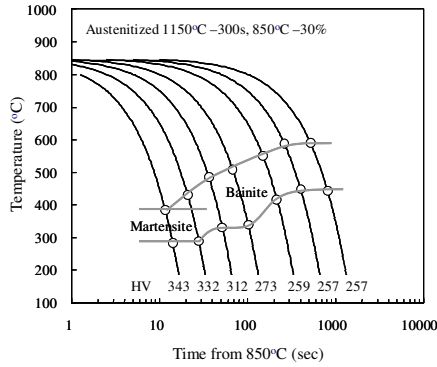


Figure 3. CCT diagram of the steel used.

### Transformation behavior during isothermal holding and the following heat treatment after accelerated cooling

In order to clarify transformation behavior of supercooled austenite during the isothermal holding after the accelerated cooling, the samples were reheated to 900°C for 300s, followed by rapid cooling to various temperatures ranging from 350 to 600°C with a cooling rate of 50°C/s, and isothermally held at each temperature for 10 to 1,000s, then quenched (Figure 4).

To investigate transformation behavior during the following heat treatment, the samples were reheated to 900°C for 300s, followed by rapid cooling to 500°C with a cooling rate of 50°C/s. Then, the samples was isothermally held at 500°C for 10s, then reheated to 650°C with a heating rate of 15°C/s and held at the temperature for 10s, followed by cooling to the ambient temperature with a cooling rate of 0.5°C/s. The other sample was accelerated cooled to 500°C and isothermally held at the temperature for 30s, then cooled to the ambient temperature with a cooling rate of 0.5°C/s for comparison (Figure 5).

Microstructural observations by scanning electron microscopy (SEM), dilatation measurements and hardness measurements were carried out in order to understand transformation behavior from supercooled austenite to bainite during the isothermal hold and the following heat treatment. To distinguish the M-A, two-stage electrical etching was conducted in metallography [20].

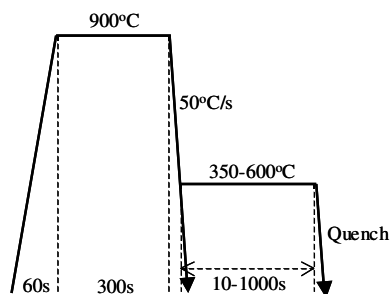


Figure 4. Heat pattern of isothermal transformation tests.

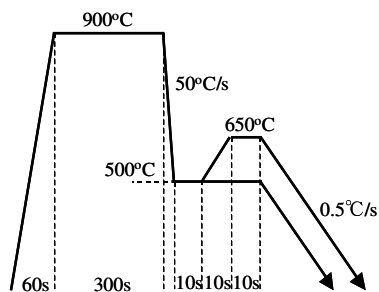


Figure 5. Heat pattern of accelerated cooling isothermal holding and reheat treatment.

## Laboratory scale hot-rolling and mechanical properties

Figure 6 shows the schematic diagram of production conditions of the laboratory hot rolled plates. The samples with 100mm in thickness were reheated to 1,150°C for 1h, followed by hot rolling to 25mm-thick plates. The finishing temperature was 850°C. The samples were accelerated cooled immediately after the hot rolling to various temperatures ranging from 400 to 600°C around the Bs (bainite start) temperature. Then, the samples were reheated from the temperatures to 650°C, and air cooled to the ambient temperature. Tensile tests and Charpy impact tests were performed to investigate microstructure-property relationships in the steels.

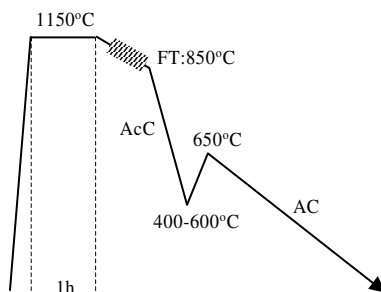


Figure 6. Schematic diagram of production conditions of laboratory scale plates.

## Results and Discussion

### Transformation Behavior during Isothermal Holding

Figure 7 shows dilatation curves during isothermal holding at 400, 500 and 600°C for 100s, after accelerated cooling with a cooling rate of 50°C/s. Marked expansion generated by transformation from austenite to bainite or martensite was observed as shown in the figures. The transformation rate at the isothermal holding at 600°C was sluggish compared with the ones at the lower temperatures, and the transformation seemed to be stagnated at the 100s holding.

Typical SEM micrographs for the samples isothermally held at 400, 500 and 600°C for 100s, followed by quenching are shown in Figure 8. Microstructure in the sample isothermally held at 400°C appeared to be mixture of lower bainite and tempered martensite (Figure 8(a)). The sample isothermally held at 500°C showed an upper bainite structure containing a large amount of M-A (Figure 8(b)). The upper bainite structure is considered to form by the isothermal transformation at the temperature. The volume fraction of M-A was about 8% in the sample. The sample isothermally held at 600°C also showed an upper bainitic structure (Figure 8(c)). However, the microstructural morphology was polygonal compared to the one isothermally held at 500°C. The volume fraction of M-A was about 20% in the sample.

As observed in the micrographs, the volume fraction of M-A increased with a rise in the isothermal holding temperature around the Bs, and the microstructural morphology became polygonal.

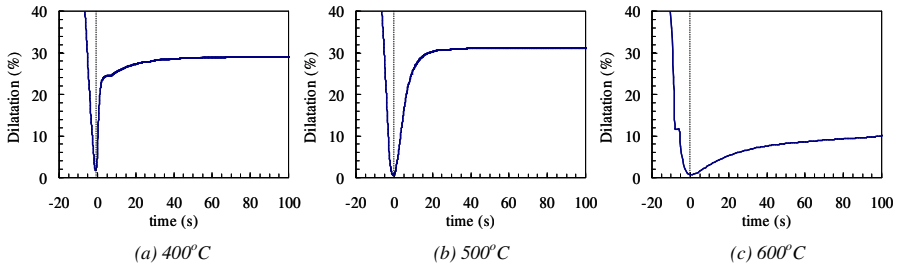


Figure 7. Dilatation curves of the steels during isothermal holding at 400, 500 and 600°C for 100sec.

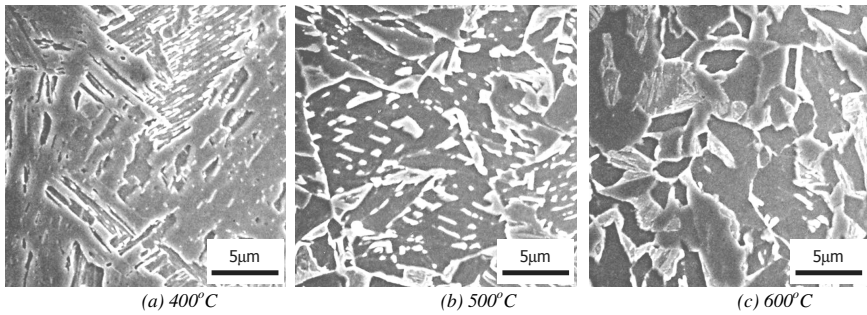


Figure 8. Microstructure of the steels after isothermal heat treatment at 400, 500 and 600°C for 100sec.

Figure 9 shows the dilatation curves after the isothermal holding and reheating. The sample directly cooling after the isothermal holding at 500°C (pattern (a)) did not show clear expansion by the transformation during cooling with the cooling rate of 0.5°C/s. On the other hand, the sample reheated at 650°C (pattern (b)) showed marked expansion at around 350°C due to the transformation.

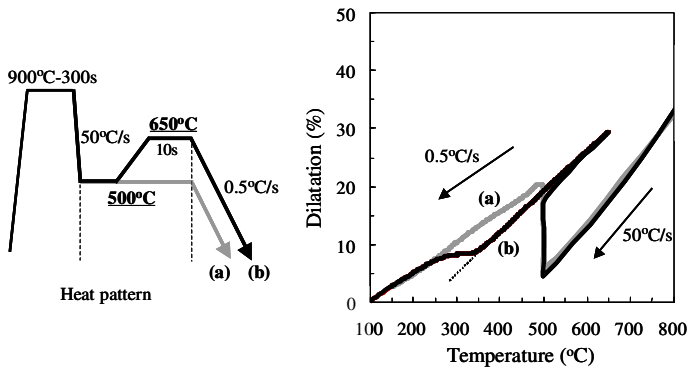
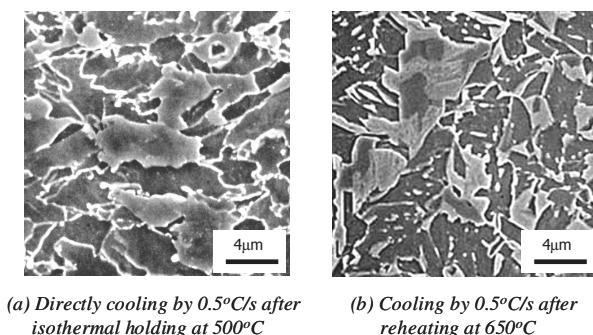


Figure 9. Dilatation curves after isothermal holding and reheating.

### Microstructural Change by Heat treatment after Accelerated Cooling and Isothermal Holding

Figure 10(a) shows a typical SEM micrograph for the sample isothermally held at 500°C, and cooled to the ambient temperature with a cooling rate of 0.5°C/s. The sample appeared to have mixed microstructure of polygonal ferrite and upper bainite containing M-A, which is seen as bright region in the micrograph. It is considered that the untransformed austenite transformed to polygonal ferrite during the slow cooling after the isothermal holding. The carbon concentration to the untransformed austenite seemed to control the transformed structure, M-A or polygonal ferrite.

Figure 10(b) shows a SEM micrograph for the sample isothermally held at 500°C, followed by heating to 650°C and cooling to the ambient temperature with a cooling rate of 0.5°C/s. A large amount of M-A observed in the sample suggests that the most of untransformed austenite transformed to M-A during the slow cooling to the ambient temperature, due to highly concentrated carbon into the untransformed austenite during the heat cycle.



*Figure 10. Effect of reheat treatment after rapid cooling and isothermal holding on Microstructure.*

Furthermore, the authors examined the effect of carbon distribution on the transformation behavior by reheat treatment after Accelerated Cooling and Isothermal Holding. Figure 11 shows the result of area analysis of carbon by EPMA after the isothermal holding at 500°C. Distribution of carbon is relatively homogeneous as shown in this map. On the other hand, partition of carbon is clearly observed in the sample reheated at 650°C. The carbon concentrated regions seem to be transformed to M-A, and other regions seem to be bainitic-ferrite structure. Based on these observations, we assumed that the carbon concentration to the untransformed austenite controlled the transformed structure, M-A or bainitic ferrite. In this complex process of thermal cycles, it is thought that the role of Nb is to promote the formation of M-A.



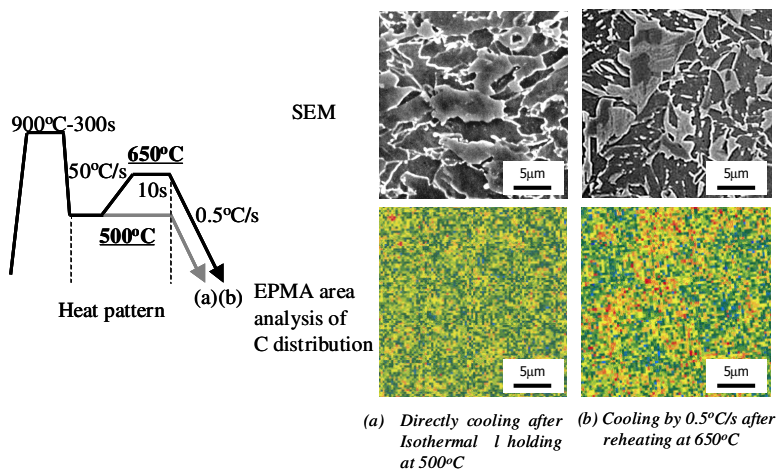


Figure 11. Effect of carbon distribution on transformation behavior.

Figure 12 shows schematic illustration of microstructural change during the heat cycle. The heat cycle consists of three stages. The first stage is the accelerated cooling to the temperature just above the  $B_s$  temperature and the isothermal holding at the temperature. At this stage, the microstructure consists of bainite and untransformed austenite. The second stage is heating from the temperature of isothermal holding to, for example, 650°C. At this stage, carbon concentrates into the untransformed austenite. The supersaturated carbon and dislocation density in bainite also decrease at this stage, simultaneously. The final stage is cooling from the heating temperature. As the carbon concentration into the untransformed austenite is high enough to be transformed to M-A, the dual phase structure of dispersed M-A in bainitic ferrite matrix can be obtained even in slow cooling.

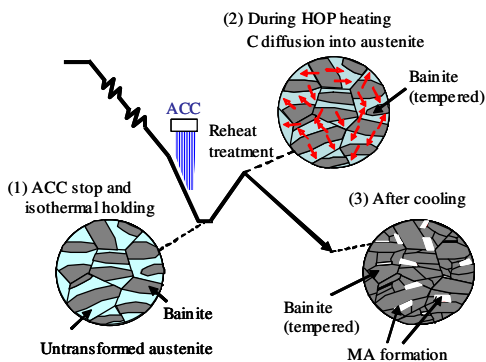


Figure 12. Schematic illustration of microstructure change in the reheat treatment for dual phase microstructural control.

### Effect of M-A on Mechanical Properties

Figure 13 shows the effect of volume fraction of M-A on tensile properties and impact toughness in 25mm-thick plates, produced by a laboratory scale hot-rolling mill with the following simulated thermal cycle. The tensile strength monotonically increased with an increase in the volume fraction of M-A. On the contrary, the yield strength decreased with an increase in the volume fraction of M-A. This is probably due to dense mobile dislocations around the M-A, which are generated by volume expansion at the transformation. As a result, the yield ratio dramatically decreased from about 90 to 65% with the increase in the volume fraction of M-A from 1 to 25%. As for the impact toughness, absorbed energy at 0°C gradually decreased from about 200 to 100J with the increase in the volume fraction of M-A. It is noted that to obtain the excellent combination of tensile properties and impact toughness, the volume fraction of M-A should be controlled to the optimal range from 5 to 15%.

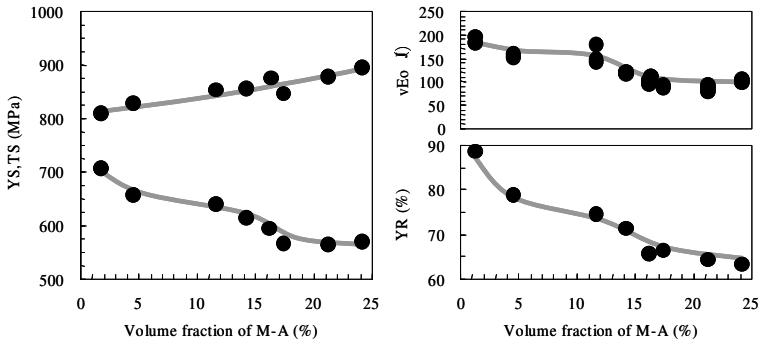


Figure 13. Effect of volume fraction of M-A on mechanical properties.

### Trial Production of Developed 780MPa Steel Plates

#### Mechanical Properties

Based on the basic research on microstructural control of the M-A and bainitic ferrite dual-phase structure, trial production of the developed 780MPa grade steel plates was made by the plate mill, combining “Super-OLAC” and “HOP”, which were installed at West-Japan Works, JFE Steel Corporation [11]. Thickness of the manufactured plates was 12, 25 and 40 mm.

Table 2 shows chemical analysis results for the produced plates. The  $C_{eq}$  and  $P_{cm}$  values of the plates were 0.54 and 0.24, respectively. Typical mechanical properties of the plates are shown in Table 3. The obtained plates satisfied the target properties in tensile and Charpy impact tests, namely, yield strength over 650MPa, tensile strength over 780MPa, yield ratio under 80% and the Charpy absorbed energy at 0°C over 70J.

Figure 14 shows typical stress-strain curves of the newly developed 780MPa grade steel plate at 40mm thickness compared against conventional plates at the same grade and thickness. The yield strength of the developed steel plate is lower than that of the conventional one, although the both curves do not show apparent Luder’s elongation. The uniform elongation of the developed plate, over 8%, is greater than that of the conventional one.

Figure 15 represents typical hardness distributions in a 25mm-thick plate through the thickness, showing quite uniform hardness distributions with hardness value of about 280 in Vickers scale (HV).

Table 2. Chemical compositions of newly developed steel plates (mass%).

C	Si	Mn	P	S	Others	Ceq	PCM
0.06	0.18	1.98	0.011	0.002	Cu, Ni, Cr, Nb, V, Ti	0.54	0.24
Ceq=C+Si/24+Mn/6+Ni/40+Cr/5+Mo/4+V/14							
PCM=C+Si/30+Mn/20+Cu/20+Ni/60+Cr/20+Mo/15+V/10+5B							

Table 3. Mechanical properties of newly developed steel plates.

t (mm)	YS (MPa)	TS (MPa)	El (%)	YR (%)	vE0°C (J)
12	688	923	23	75	188
25	703	912	33	77	216
40	665	852	36	78	199
Target	>650	>780	>16	<80	>70

Tensile test: Full thickness (JIS No.5)-transverse, Charpy test: 1/4t-transverse

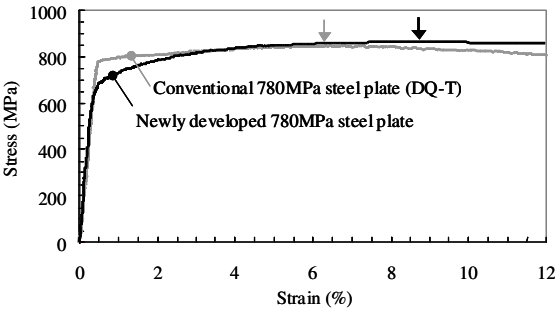


Figure 14. Typical stress-strain curve of newly developed 780MPa steel and conventional 780MPa steel.

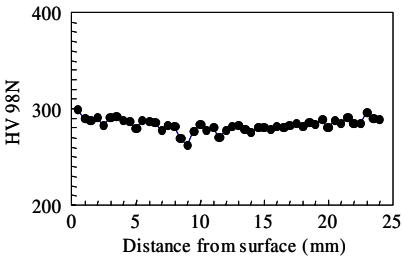


Figure 15. Typical hardness distribution of 25mm steel plate through the thickness.

Weldability

Figure 16 shows the maximum hardness test results for the 25mm-thick plate, which was performed in accordance with the JIS standards (JIS Z 3101). The maximum hardness increased with a decrease in the bead length. Although the maximum hardness at the bead length of 0 (arc strike) was 356HV, the maximum hardness values with bead length over 10mm were under 350HV. These low values in the maximum hardness tests as 780MPa grade plates are attributed to the alloy design with the low carbon content and Ceq value.

Table 4 shows the y-groove weld cracking test results for the 25mm- and 40mm-thick plates, which was performed in accordance with the JIS standards (JIS Z 3158). According to the test results, the preheat temperature to avoid cold cracking in CO<sub>2</sub> welding is 25°C or lower, showing excellent weldability of the plates.

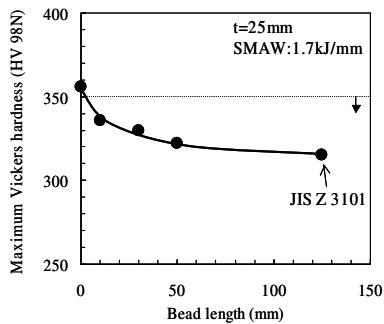


Figure 16. Result of maximum hardness test for 25mm steel plate.

Table 4. Results of y-groove weld cracking tests for 25 and 40mm steel plates.

Welding condition	t (mm)	Preheating temperature (°C)	Cold crack retio (%)		
			Surface	Root	Cross section
CO2 welding Welding consumable :MG-80 Heat input:1.7kJ/mm Atmosphere:20°C-60%	25	25	0	0	0
		50	0	0	0
	40	25	0	0	0
		50	0	0	0

Performance of Welded Joint

Since CO<sub>2</sub> welding and SAW (sub-merged arc welding) are mostly used in joining "diaphragm"- "column" and "column"- "column" in building construction, mechanical properties of welded joints by CO<sub>2</sub> welding and SAW welded under the typical conditions were examined. Table 5 shows tensile and Charpy impact test results for the welded joint by CO<sub>2</sub> welding with heat input of 2.1kJ/mm. The mechanical properties were satisfactory, with tensile strength over 780MPa, and impact energy at 0°C over 70J for all the notch position.

Table 6 shows tensile and Charpy impact test results for the welded joint by SAW with heat input of 4.6kJ/mm. The excellent properties were also obtained in this welded joint, with tensile strength over 780MPa, and impact energy at 0°C over 70J for all the notch position.

Table 5. Welding conditions and mechanical properties of CO<sub>2</sub> welded joint.

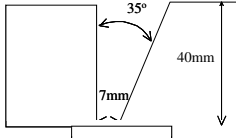
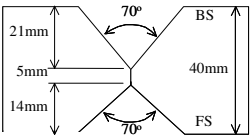
t (mm)	Shapes and dimensions of groove	Welding conditions	Tensile properties		Charpy impact properties	
40		Welding consumable : MG-80 Heat input: 2.1kJ/mm Preheat: None Inter pass temp: <150°C	TS (MPa)	Fracture position	Notch position	vE0°C (J)
			804 806	WM WM	WM	97
					FL	79
					HAZ1mm	174
					HAZ3mm	270

Table 6. Welding conditions and mechanical properties of SAW welded joint.

t (mm)	Shapes and dimensions of groove	Welding conditions	Tensile properties		Charpy impact properties	
40		Welding consumable : US-80BN - PFH80AK Heat input: 4.6kJ/mm Preheat: 50°C Inter pass temp: <250°C	TS (MPa)	Fracture position	Notch position	vE0°C (J)
			817 816	WM WM	WM	87
					FL	86
					HAZ1mm	231
					HAZ3mm	250

## Conclusions

(1) High strength steel plates with 780MPa in tensile strength, which were suitable for building construction taking seismic design into account, have been developed. The steel plates have excellent combination of high strength, toughness, low yield ratio and weldability. The key technology to obtain the excellent combination in mechanical properties is the microstructural control of the M-A (martensite-austenite constituent) and bainitic ferrite dual-phase structure, through the on-line heat treatment immediately after the accelerated cooling. The developed steel plates have microstructure of fine M-A particles dispersed in the bainitic ferrite matrix.

(2) Trial production of the developed 780MPa grade steel plates was made by the actual plate mill, combining “Super-OLAC” and “HOP”. The obtained plates showed excellent mechanical properties, with yield strength over 650MPa, tensile strength over 780MPa, yield ratio under 80%, uniform elongation over 8% and Charpy impact energy over 70J at 0°C.

(3) The excellent weldability of the developed 780MPa grade steel was confirmed by the maximum hardness test and y-groove weld cracking test performed in accordance with the JIS. Mechanical properties of welded joints made by CO<sub>2</sub> welding and SAW were also

satisfactory, with tensile strength over 780MPa, and impact energy at 0°C over 70J for all the notch position.

## References

- [1] Y. Kaneko, N. Shikanai, T. Shiraga, T. Kojima, S. Yamamoto, and M. Katahira, NKK's Structural Steels, *NKK Technical Review*, Vol.140, 1992, p.1-10
- [2] M. Ohashi, H. Mochizuki, T. Yamaguchi, Y. Hagiwara, H. Kuwamura, Y. Olamura, Y. Tomita, N. Komatsu, and Y. Funatsu, Development of New Steel Plates for Building Structural Use, *Seitetsu Kenkyu*, Vol.334, 1989, p.17-28
- [3] H. Hatano, H. Kawano, S. Okano, 780MPa Class Steel Plate for Architectural Construction, *Kobe Steel Engineering Reports*, Vol.54, No.2, 2004, p.105-109
- [4] Y. Kamada, Y. Ichinohe, F. Ohtake, K. Kawano, and K. Ohnishi, High Strength Low Yield Steel Plates for Building Use (HT590, Ht780), *Sumitomo Met.*, Vol.43, No.7, 1991, p.13-22
- [5] N. Shikanai, H. Kagawa, M. Kurihara, and H. Tagawa, Influence of Microstructure on Yielding Behavior of Heavy Gauge High Strength Steel Plates, *ISIJ International*, Vol.32, No.3, 1992, p.335
- [6] K. Satoh, M. Toyoda, M. Tsukamoto, I. Watanabe, H. Tagawa, and S. Tsuyama, Influence of Yield Ratio of Steels on Structural Performance, *Quarterly Journal of the Japan Welding Society*, Vol.3, No.3, 1985, p.153-159
- [7] M. Toyoda, Significance of Tensile Deformation Properties of Steels for Framed Structures, *Journal of the Japan Welding Society*, Vol.58, No.7, 1989, p.15-20
- [8] K. Hayashi, S. Fujisawa, and I. Nakagawa, High Performance 550MPa Class High Strength Steel Plates for Buildings, *JFE Technical Review*, No.5, 2004, p.45-50
- [9] Y. Murakami, S. Fujisawa, and K. Fujisawa, The Features of New High-strength Steel Materials "550N/mm<sup>2</sup> Class" for Building Frames, *JFE Technical Review*, No.10, 2005, p.35-40
- [10] K. Omata, H. Yoshimura, and S. Yamamoto, The Leading High Performance Steel Plates with Advanced Manufacturing Technologies, *NKK Technical Review*, Vol.179, 2002, p.57-62
- [11] A. Fujibayashi, and K. Omata, JFE Steel's Advanced Manufacturing Technologies of Leading High Performance Steel Plates, *JFE Technical Review*, No.5, 2004, p.8-12
- [12] M.E. Bush, and P.M. Kelly, Strengthening Mechanisms in Bainitic Steels, *Acta Met.*, No.19, 1971, p.1363
- [13] V. Biss, and R.L. Cryderman, Martensite and Retained Austenite in Hot-Rolled, Low-Carbon Bainitic Steels, *Met. Trans.*, No.2, 1971, p.2267
- [14] J. Gerbase, J.D. Embury, and R.M. Hobbs, Structure and Properties of Dual-Phase Steels, *Metallurgical Society of AIME*, edited by R.A. Kot, and J.W. Morris, 1979, p.183
- [15] R. Stevenson, Formable HSLA and Dual-Phase Steels, *Metallurgical Society of AIME*, edited by R.A. Kot, and J.W. Morris, 1979, p.99
- [16] A.P. Coldren, R.L. Cryderman, et al, *Steel Strengthening Mechanism*, Zurich, Climax

Molybdenum, 1969, p.17-44

[17] L.J. Habraken, and M. Economopoulos, *Transformation and Hardenability in Steels*, Mich, No.109, 1967, p.69

[18] M. Okatsu, T. Shinmiya, N. Ishikawa, and S. Endo, Development of High Strength Linepipe with Excellent Deformability, *Proceedings of OMAE'05*, 2005, OMAE2005-67149

[19] N. Ishikawa, M. Okatsu, S. Endo, and J. Kondo, Design Concept and Production of High Deformability Linepipe, *Proceedings of IPC2006*, 2006, IPC2006-10240

[20] H. Ikawa, H. Oshige, and T. Tanoue, Study on the Martensite-Austenite Constituent in Weld-Heat Affected Zone of High Strength Steel, *Journal of the Japan Welding Society*, Vol.49, No.7, 1980, p.47-52